Shell-model plus Hartree-Fock calculations for the neutron-rich Ca isotopes

B. A. Brown
Department of Physics and Astronomy, and National Superconducting Cyclotron Laboratory, Michigan State University, East Lansing, Michigan 48824-1321
and Department of Physics, University of Stellenbosch, Stellenbosch 7600, South Africa

W. A. Richter
Department of Physics, University of Stellenbosch, Stellenbosch 7600, South Africa
(Received 1 May 1998)

A new method is developed to combine the large-basis shell-model and Hartree-Fock methods. The Hartree-Fock method is used to obtain the absolute uncorrelated binding energies, a starting set of single-particle energies, and the single-particle radial wave functions. The shell model Hamiltonian is modified to remove the monopole terms and these are replaced by Hartree-Fock single-particle energies. The shell model is then used to calculate the ground-state correlation energy and the excited state spectrum. Applications are made to the nuclei $^{47-60}$Ca. A detailed comparison is made for ^{48}Ca including the electron scattering data for ^{48}Ca. [S0556-2813(98)04410-0]

PACS number(s): 21.60.Cs, 21.60.Jz, 27.40.+z

I. INTRODUCTION

Nuclear structure properties are mainly determined by the spacing of the single-particle states in the mean field. A sufficiently large gap in the spacing between spherical energy levels gives rise to a closed-shell structure when the levels are filled up to the gap. The properties of these closed-shell nuclei and those around it are dominated by the single-particle degrees of freedom. When the levels are closely spaced, various collective properties associated with the scattering and correlation of the nucleons among the closely spaced levels are important. This leads to BCS correlations for identical nucleons and to vibrational and deformed correlations between valence protons and neutrons.

In a spherical shell-model calculation one starts out near one of the closed-shell nuclei, and the collective properties evolve as valence nucleons are added. A typical example is the sd shell [1] where one finds that the properties of deformed nuclei such as ^{20}Ne and ^{24}Mg as well as rather spherical nuclei such as ^{34}Si are all reproduced by a single mass-dependent effective shell-model Hamiltonian.

In such shell-model calculations one usually starts out with a set of single-particle energy levels which are determined from one-nucleon transfer reactions on the initial closed-shell nucleus (^{16}O for the sd shell). As one adds valence nucleons, these single-particle energies are modified by the valence shell-model interaction and evolve as a function mass.

Perhaps the most important problem with such shell-model calculations is to ensure that the variation of the single-particle energies (SPE's) with mass reproduces the observed trends in the single-particle data. The variation of the SPE's with mass is complicated. One might expect that it is given by an underlying mean-field Hamiltonian. However, they are also influenced by intruder states. By ''intruder state'' we refer to those configurations which are not included explicitly in the model space, but which are low lying and will thus mix with and have an indirect effect on the spectra. The nature of these intruder states depends upon mass and neutron excess. For example, the properties of nuclei near $N=Z$ are strongly influenced by the intruder states which involve three- and four-body (alpha) cluster configurations.

When one starts out with a microscopic residual interaction such as the renormalized G matrix of Kuo and Brown, the calculated properties of the nuclei with a few valence particles are usually in reasonable agreement with experiment. But as one adds many valence particles the comparison with experiment diverges. An example of this can be observed in the calculations of McGrory, Wildenthal, and Halbert [2] for $^{42-50}$Ca with the renormalized Kuo-Brown G matrix [3] and with the SPE's observed for ^{41}Ca. The spectrum obtained for ^{48}Ca with this interaction is totally different from experiment. The same problem occurs also for the more recent G matrix calculations [4]. The reason for this problem is that the SPE's appropriate for ^{48}Ca are not correctly reproduced. As suggested above, the reason why the SPE mass dependence predicted by the G matrix does not correspond to experiment is nontrivial. It is not necessarily a defect of the G matrix, but may be more related to the degree of sd-shell closure as one goes from ^{40}Ca to ^{48}Ca.

The traditional approach to correcting this behavior has been to modify the two-body matrix elements in such a way as to ensure that the behavior of the SPE's as a function of mass is correct. For the Ca isotopes, this was done in Ref. [2] for those fp-shell matrix elements which involve the $f_{7/2}$-$p_{3/2}$ interaction and then in Ref. [5] for those matrix elements which involve the $f_{7/2}$-$f_{5/2}$ interaction. These modifications are not necessarily fundamental in nature, and the corrections which one applies in one particular situation may not be applicable to the general case.

A more recent example of this problem can be found in the comparison of the applications of the FPD6 and KB3 interactions to Monte Carlo calculations of the ^{56}Ni spectrum [6] and to their application in nuclei above ^{56}Ni [7]. The KB3 interaction is a version of the Kuo-Brown G matrix in

which the monopole components of both the $T=0$ and $T=1$ parts of the interaction have been modified [8]. The FPD6 interaction is a purely phenomenological interaction in the form of a ''modified one-boson-exchange potential'' [9] whose parameters where determined from fp-shell data in the mass region $A=41-49$ [10]. The ''modified'' aspect of the FPD6 interaction refers to the monopole terms. Thus both of these interactions take into account the empirical change of the SPE's in the lower part of the fp shell. When one reaches ^{56}Ni in the Monte Carlo calculations, the FPD6 works better than the KB3, mainly because the extrapolated SPE's are better. However, both KB3 and FPD6 are better than the renormalized G matrix without any monopole corrections. The monopole additions to KB3 and FPD6 are not derived from fundamental considerations, but are simply put in to achieve agreement with experiment.

Thus, it would be important to have a more reliable and general procedure for ensuring that the evolution of the SPE's with mass is under control. In this paper we approach this problem by combining the large-basis shell-model (SM) calculations with the Hartree-Fock (HF) method. Specifically by the HF method we mean a spherical HF calculation carried out for a given nucleus usually under the assumption that the orbits are occupied in their lowest-energy states. The HF method does not include BCS or deformation correlations since they will be part of the SM aspect. A SM calculation means that the Hamiltonian matrix corresponding to all possible Slater determinants for the closely spaced valence orbitals is diagonalized to obtain the wave functions and correlation energies.

The HF method will be used to obtain the uncorrelated binding energy as well as the SPE's for a given nucleus. The shell-model Hamiltonian is then modified in order to remove the monopole terms which are responsible for changing the SPE's within the valence interactions, and these are replaced by the HF SPE's. Diagonalization of the shell-model Hamiltonian gives the correlated wave functions for the ground and excited states, including the correlation energy for the ground state.

Our modified procedure also deals with another defect of carrying out shell-model calculations for a large number of valence particles. It is well known from the Skyrme interaction [11] that one needs a repulsive three-body or density-dependent interaction to account for the saturation of nuclear matter. Most of this repulsive interaction is related to the higher-order corrections needed when the shell-model space is truncated to a single Slater determinant for the spherical closed-shell nuclei, although some of it may also be due to an underlying three-nucleon interaction. On the other hand, the SM calculations are usually carried out with only a two-body interaction which is not explicitly density dependent. Thus the evolution of binding energy with mass and its relationship to the SPE's is different for the HF and SM methods, and should be more accurately and fundamentally taken into account by the HF method.

In order to incorporate the HF SPE's as a function of mass number, the diagonal monopole interaction is first removed and then the SPE's are inserted. The monopole terms have the form

$$V_m(j_1,j_2)=\frac{\sum_J (2J+1)\langle j_1,j_2,J|V|j_1,j_2,J\rangle}{\sum_J (2J+1)}. \quad (1)$$

The modified two-body matrix elements with the monopole terms removed are

$$\langle j_1,j_2,J|V|j_1,j_2,J\rangle^*=\langle j_1,j_2,J|V|j_1,j_2,J\rangle-V_m(j_1,j_2). \quad (2)$$

The modified interaction SM* has the property that the total interaction energy for any closed-subshell configuration as well as the total closed-shell configuration is zero. It also has the property that the SPE's for the ''hole'' states in the closed-shell minus one-nucleon system is the same as for the initial one-particle SPE's.

It appears that we may remove more information in Eq. (1), ten terms for the various j_1,j_2 combinations, than are replaced by the four SPE's. However, the complete set of ten monopole energies is related to the configuration (occupation number) dependence of the SPE's in the Hartree-Fock method. As mentioned above, since the Hartree-Fock method accounts for saturation via the density-dependent interactions, it may be that the configuration dependence of the SPE's is better described in the HF method than from the shell-model two-body matrix elements of Eq. (1). However, for this study we take a configuration-independent set of SPE's which are those obtained in the Hartree-Fock method with the simplest $f_{7/2}^8$ configuration for ^{48}Ca (and equivalent simple configurations for other Ca isotopes). Since the wave functions for the Ca isotopes are dominated by these simple configurations, the rearrangement terms associated with the change in the SPE's with configuration are typically only a few hundred keV, and are small compared to the other uncertainties in the HF and SM calculations. However, in other situations where the configuration mixing is much larger, e.g., for ''deformed'' states, it may be more important to take into account the configuration dependence of the SPE's.

In this paper we consider the application of the SM + HF approach to the neutron-rich Ca isotopes. We consider two fp-shell residual interactions. The renormalized G matrix of Kuo and Brown (KB) [3], and the FPD6 interaction [10] discussed above which will be abbreviated by D6. The versions of these interactions with the monopole removed and with the HF SPE added will be denoted generically by SM* + HF and, specifically in our examples, by KB* + HF and D6* + HF.

For the HF part of the calculation we use the Skyrme interaction. Since the introduction of the Skyrme interaction by Vautherin and Brink [11], this parametrization has proved remarkably useful and successful for HF calculations. It appears to incorporate the essential physics in terms of a minimal parametrization, e.g., an s- and p-wave expansion of an effective nucleon-nucleon interaction together with a density-dependent part which accounts for the truncation of the shell-model space to a closed-shell configuration as well as for three-body interactions. Since the interaction is phenomenological, the parameters need to be determined from experimental data. Rather good results for the total binding energies and SPE's can be obtained when the Skyrme param-

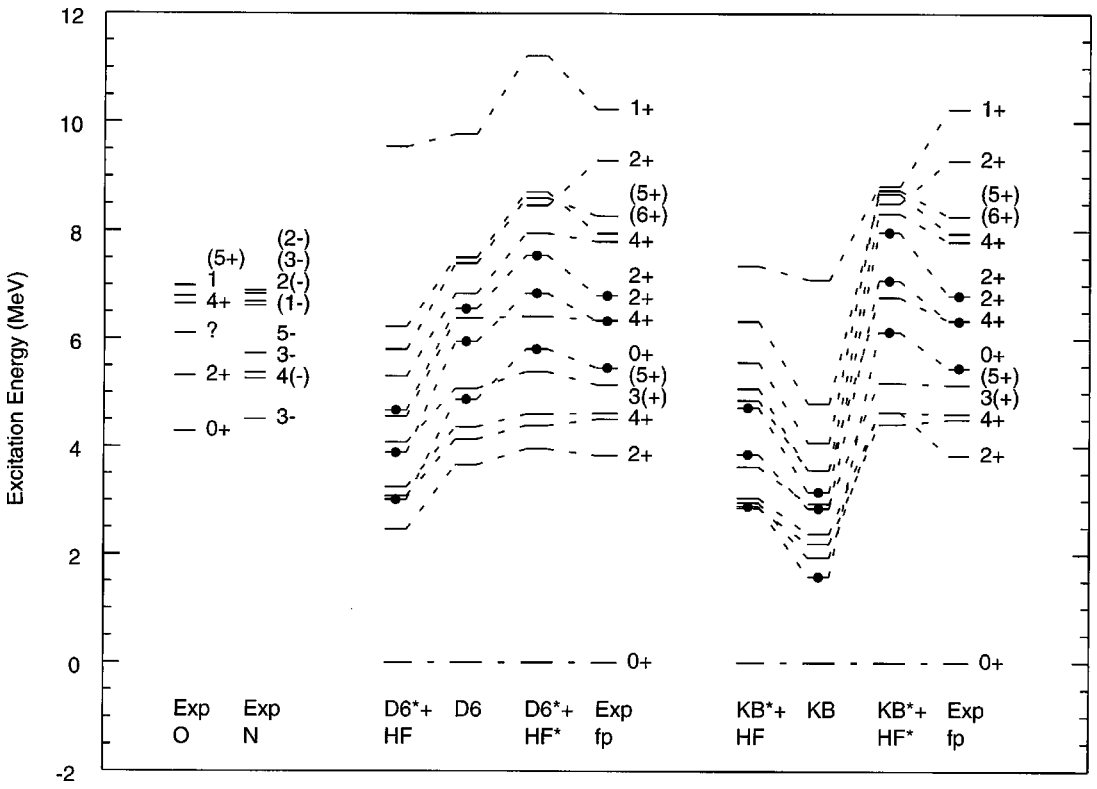

FIG. 1. Energy levels for ^{48}Ca. See text for a discussion of the labels.

eters are fitted to experimental data. Here we used the SKX set of parameters [12] obtained from considering the properties for the spherical nuclei ^{16}O, ^{24}O, ^{34}Si, ^{40}Ca, ^{48}Ca, ^{48}Ni, ^{68}Ni, ^{88}Sr, ^{100}Sn, ^{132}Sn, and ^{208}Pb, as well as some nuclear and neutron matter properties.

As alluded to above, the HF results are not always in good agreement with the properties of the closed-shell nuclei, and the use of HF SPE's does not in itself solve the problem of the influence from intruder states. For the SKX interaction the agreement between the HF and experimental SPE was considerably worse for ^{16}O and ^{40}Ca as compared to those nuclei such as ^{48}Ca with a neutron excess. This may be related to the fact that as many valence particles are added to the active model space, the low-lying intruder configurations become Pauli blocked and the HF single-particle energies may be more reliable.

Although the HF SPE's should be a reasonable starting point, one might expect that the actual SPE's for a given nucleus may differ from those given by a particular HF calculation. Thus, for our example, we consider a modification of the HF SPE's which are derived from matching the binding energy (BE) differences BE(48)$-$BE(47) for the $f_{7/2}$ orbital and BE(49)$-$Be(48) for the $p_{3/2}$, $p_{1/2}$, and $f_{5/2}$ orbitals. ''BE'' represents the binding energy of the ground state of ^{49}Ca for $p_{3/2}$, the first excited state for $p_{1/2}$, and the third excited state for $f_{5/2}$. This selection of levels is based upon the large spectroscopic factors observed in one-nucleon transfer reactions [13]. In particular, the second exited state of ^{49}Ca which is $5/2^-$ is weak in the (d,p) reaction [13] and it is the third excited state which is also $5/2^-$ which is dominated by the ^{48}Ca(0^+) plus $f_{5/2}$ configuration [the second excited state in ^{49}Ca has the structure ^{48}Ca(2^+) plus $p_{3/2}$]. The final interactions are denoted generically by SM* + HF* and, specifically in our example, by KB* + HF* and D6* + HF*.

In the following sections we first concentrate on the properties of ^{48}Ca and how they depend upon the various models. In Sec. II we discuss the general level scheme for ^{48}Ca and in Sec. III we discuss some details related to the electron scattering data. Then we use the D6* + HF* model to study the more neutron-rich Ca isotopes, to make comparisons to the few data available, and to make some predictions for the other nuclei which may be studied in future radioactive-beam experiments.

All of the results are obtained with the shell-model code OXBASH [14] in the full fp-shell model space. Contrary to the impression given by Ref. [15], the full fp-shell calculations are straightforward for all of the Ca isotopes.

II. LEVEL SCHEME FOR ^{48}Ca

The experimental and theoretical levels for ^{48}Ca are shown in Fig. 1. The experimental data are divided into three parts: ''Exp-fp,'' those positive parity levels which can be assigned to the $(fp)^8$ configurations; ''Exp-N,'' other levels which are probably negative parity; and ''Exp-O,'' other levels which are positive parity or not known. All of the experimental and theoretical levels are shown up to 7 MeV. Above 7 MeV only some selected levels related to the $(fp)^8$ configuration are shown.

The theoretical levels for ^{48}Ca are given for SM, SM* + HF, and SM* + HF*, where SM is either D6 or KB. Although there are many levels experimentally identified in ^{48}Ca, their spins and their associations with the fp-shell configurations are often ambiguous. We are guided mainly by the comparison of the theoretical electron scattering form

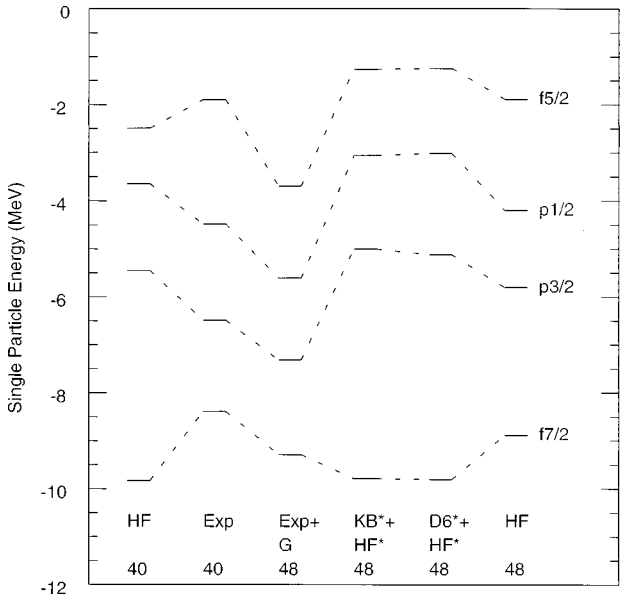

FIG. 2. The SKX HF and SM*+HF* single-particle energies for ^{40}Ca and ^{48}Ca.

factors to experimental data which is discussed in detail in Sec. III. The levels which are identified in this way have a predominantly one-particle–one-hole (1p-1h) structure relative to the predominantly $(f_{7/2})^8$ configuration for the ^{48}Ca ground state.

In addition to those states determined from electron scattering there are states observed strongly in the ^{46}Ca(t,p) reaction [16]: 5.46 MeV 0^+, 6.33 MeV 2^+, and 6.79 MeV 2^+. The strong population of these states in (t,p) indicates their neutron 2p-2h structure, and they are associated with theoretical states which have large neutron 2p-2h components relative to a $(f_{7/2})^8$ ground state configuration for ^{48}Ca. The states which are theoretically and experimentally predominantly 2p-2h in structure are indicated by the solid circles in Fig. 1. The electron scattering form factors to these states are small compared to the those which are predominantly 1p-1h in structure. The neutron 2p-2h states for 4^+ start at 8.24 MeV, which is consistent with the start of several unidentified states at this energy in the (t,p) reaction [16].

The only known positive parity states below 7 MeV which cannot be associated with fp configurations are those shown on the left-hand side of Fig. 1: the experimental states 4.28 MeV 0^+, 5.31 MeV 2^+, and 6.65 MeV 4^+. These are most probably associated with the proton 2p-2h states, with the two protons being excited from the sd shell to the fp shell.

The HF, D6*+HF*, and KB*+HF* SPE for ^{48}Ca are compared on the right-hand side of Fig. 2. Comparison of D6*+HF* and KB*+HF* shows that the deduced SPE's for ^{48}Ca do not depend much on the residual interaction. The HF SPE's calculated with the SKX interaction are close to the empirical SM*+HF* SPE's. However, some adjustment is necessary, namely, about a 1.0 MeV shift downward for the p states and an increase in the spin-orbit splitting for the f states. For the ^{48}Ca spectrum the gap between the $f_{7/2}$ and the other orbitals is important, and HF* differs from HF in about a 1.5 MeV increase in this gap.

On the left-hand side of Fig. 2 we show the experimental SPE's for ^{40}Ca as deduced from the lowest levels in ^{41}Ca which are used for shell-model calculations in the fp shell [4,10]. They are compared with the HF SKX SPE's. The SKX SPE's are particularly bad for ^{40}Ca, and we attribute this to core breaking and intruder states near ^{40}Ca.

In addition we show in Fig. 2 (Exp+G,48) the SPE's for ^{48}Ca which are obtained from the experimental ^{40}Ca SPE's plus the centroid shifts calculated with the renormalized G matrix of Kuo and Brown [3]. It is the small spacing between the $f_{7/2}$ and the $p_{3/2}$ orbitals in the Exp+G result which leads to the problem in ^{48}Ca.

The very poor agreement with experiment with KB which was originally noted in Ref. [2] is greatly improved with KB*+HF and KB*+HF*. The fairly good agreement with experiment for D6 is improved with D6*+HF* but is somewhat worse for $D6$*+HF. We conclude (1) that it is preferable to start the shell-model calculations for a given many particle nucleus with the SM*+HF approach and (2) that they may be further improved by consideration of the single-particle and single-hole states in the neighboring odd-even nuclei.

Comparison of the D6*+HF* and KB*+HF* spectra with experiment concentrates on the ''residual'' interaction aspects of the calculations. Although KB* is not in bad agreement with experiment, D6* is considerably better. The exceptions are for the highest 2^+ and 1^+ states which are dominated by the $(f_{7/2})^{-1}$ $f_{5/2}$ configuration.

III. ELECTRON SCATTERING FROM ^{48}Ca

Inelastic electron scattering on ^{48}Ca [17] is one of the key experiments in making the association between experimental and theoretical energy levels. We have used the shell-model multiparticle transition densities (OBTD's) together with the SKX HF single-particle radial wave functions to calculate the longitudinal and transverse electron scattering form factors. Details of the form-factor calculations are described in Ref. [18]. [For comparison to the experiment of Ref. [17] we use the Donnelly-Walecka normalization as described in the text following Eq. (3) of Ref. [18].] The longitudinal form factors are obtained with a neutron effective charge of 0.64 [10] and combined with the Tassie form for the core polarization [18]. In the following discussion we will compare the experimental level scheme with that obtained with the D6* +HF* interaction.

The theoretical states which are associated with those observed in the electron scattering all have wave functions which are dominated by 1p-1h components. In particular there are three multiplets in the theoretical spectrum: a $(2,3,4,5)^+$ multiplet near 5 MeV which is mainly $(f_{7/2})^{-1}$ $p_{3/2}$, a $(3,4)^+$ multiplet near 6 MeV which is mainly $(f_{7/2})^{-1}$ $p_{1/2}$, and a $(1,2,3,4,5,6)^+$ multiplet near 9 MeV which is mainly $(f_{7/2})^{-1}$ $f_{5/2}$. Experimental candidates can be identified for most of these states.

The theoretical longitudinal form factor (LFF) for the lowest 2^+ state (see Fig. 3) is strong and is in excellent agreement in strength and shape with experiment [17]. There is no other 2^+ state identified in the experimental electron scattering until 9.29 MeV. The next largest theoretical LFF is for the fifth theoretical state at 8.46 MeV which is part of the

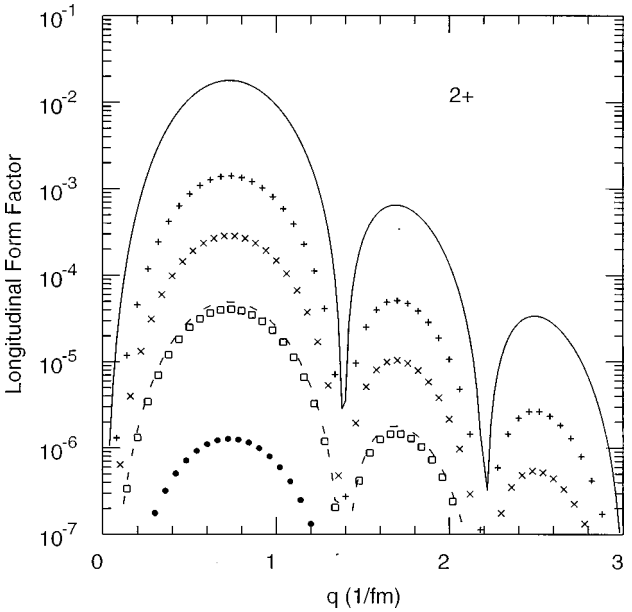

FIG. 3. Longitudinal electron scattering form factors for the lowest six 2^+ states for ^{48}Ca obtained with the D6*+HF* interaction. The levels are 3.95 MeV (solid line), 6.84 MeV (dashed line), 7.54 MeV (dots), 8.36 MeV (crosses), 8.46 MeV (pluses), and 9.30 MeV (squares).

$(f_{7/2})^{-1}$ $f_{5/2}$ multiplet. The agreement between the experimental and theoretical LFF's magnitudes is good.

The experimental LFF for the lowest 4^+ state was unresolved from that of the nearby 3^- state. Above this, four 4^+ states were identified in the experiment. The two strongest of these at 6.34 MeV and 7.79 MeV have LFF which are in good agreement (see Fig. 4) with the second and third theoretical 4^+ states. These are members of the $(f_{7/2})^{-1}$ $p_{1/2}$ and $(f_{7/2})^{-1}$ $f_{5/2}$ multiplets, respectively. The two weaker 4^+

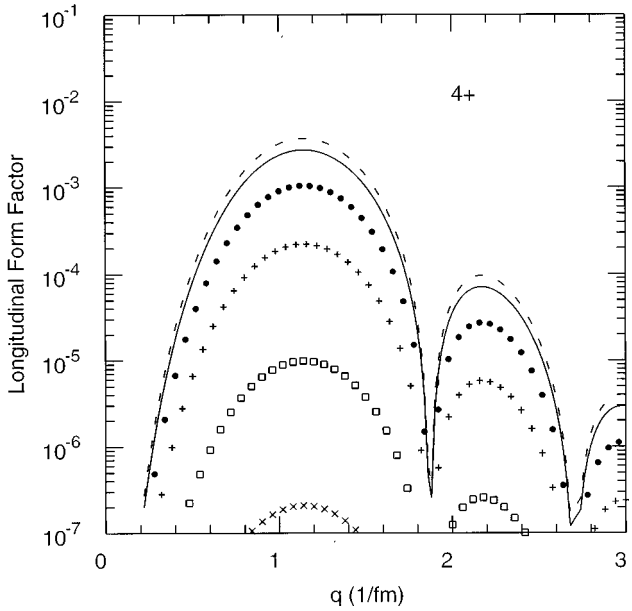

FIG. 4. Longitudinal electron scattering form factors for the lowest six 4^+ states. The levels are 4.39 MeV (solid line), 6.41 MeV (dashed line), and 7.95 MeV (dots), 8.24 MeV (crosses), 8.48 MeV (pluses), and 9.05 MeV (squares).

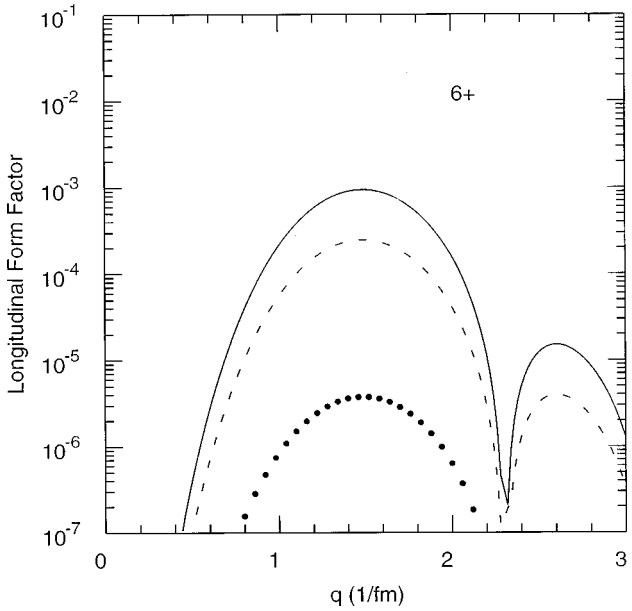

FIG. 5. Longitudinal electron scattering form factors for the lowest three 6^+ states. The levels are 8.60 MeV (solid line), 8.62 MeV (dashed line), and 9.56 MeV (dots).

states observed at 6.65 and 7.58 MeV cannot reasonably be associated with any theoretical counterpart near these energies, and we assume that they are related to proton 2p-2h configurations whose LFF strength may come from some mixing with the nearby fp-shell states.

There were no 6^+ LFF's reported in Ref. [17]. The theoretical LFF for the lowest 6^+ (see Fig. 5) at 8.60 MeV corresponding to a member of the $(f_{7/2})^{-1}$ $f_{5/2}$ multiplet is relatively large. Perhaps this could be related to the experimental state at 8.27 MeV whose spin was suggested to be 4^+ or 5^- (the experimental LFF for this state is not given in Ref. [17]). We will make this a tentative association, indicated by the (6^+) label in Fig. 1.

Next we consider the transverse form factors (TFF's) which are shown in Figs. 6–8. Only one 3^+ TFF was experimentally identified for a state at 4.61 MeV. Its shape and magnitude are in good agreement with the lowest theoretical 3^+ state at 4.60 MeV (see Fig. 7) which is a member of the $(f_{7/2})^{-1}$ $p_{3/2}$ multiplet. Likewise the 5^+ TFF observed for a state at 5.14 MeV is in excellent agreement with the theoretical state at 5.39 MeV shown in Fig. 8 which is also part of the $(f_{7/2})^{-1}$ $p_{3/2}$ multiplet. The theoretical TFF's for the higher 3^+ states are weaker. The theoretical TFF for the second 5^+ state at 8.71 MeV is strong and has a very different shape than that of the lowest state. This second theoretical state is a member of the $(f_{7/2})^{-1}$ $f_{5/2}$ multiplet and the reason for the change in shape is that the l value changes in the former but not in the latter, and because these two configurations are not strongly mixed. There is a TFF observed experimentally for a state at 7.95 MeV which is suggested to be $(2^-,6^-)$. However, its shape and magnitude are also in fair agreement with the second theoretical 5^+ state, and thus we make this tentative assignment for the comparison shown in Fig. 1.

The TFF's for the 1^+ states and their associated $B(M1)$ values have been investigated in a separate low-momentum transfer experiment [19]. Although there are many 1^+ states

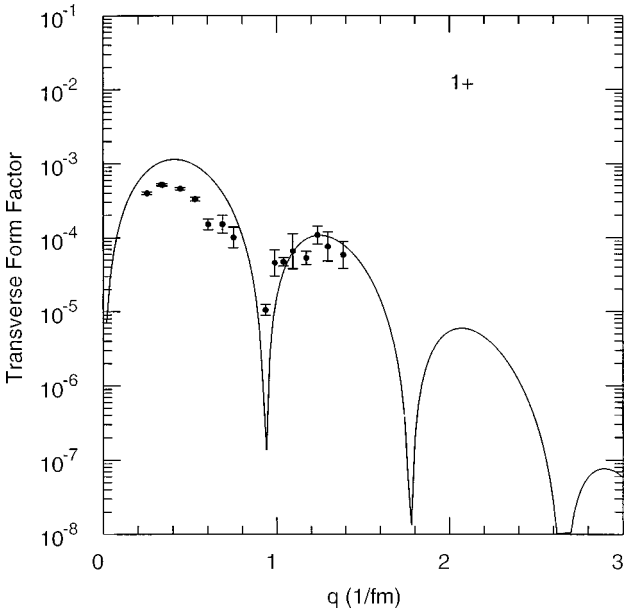

FIG. 6. Transverse electron scattering form factors for the strong (sixth) 1^+ state at 11.21 MeV. It is compared with the experimental results for the 10.23 MeV state from Ref. [19]. The theoretical form factors for the lower five states are smaller by one to two orders of magnitude.

identified starting at 7.696 MeV, the $M1$ strength is dominated by a strong state at 10.23 MeV with $B(M1)=3.9\mu_N^2$. This pattern is consistent with the present D6* +HF* calculation with the lowest 1^+ state at 8.27 MeV and the strongest $M1$ strength in a state at 11.21 MeV with $B(M1)=7.4\mu_N^2$ (obtained with the free-nucleon operator). The additional $M1$ strength fragmented over ten states between 8 and 13 MeV is $2.0\mu_N^2$. The 1^+ state with the large $M1$ strength is a member of the $(f_{7/2})^{-1}\ f_{5/2}$ multiplet (this

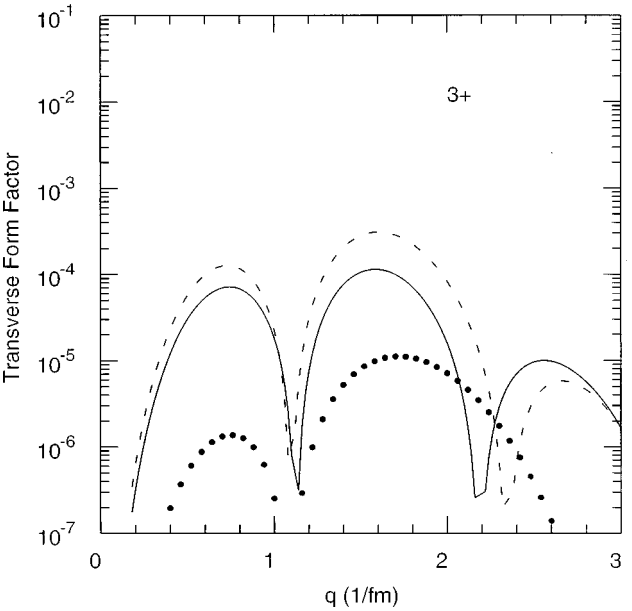

FIG. 7. Transverse electron scattering form factors for the lowest three 3^+ states. The levels are 4.60 MeV (solid line), 7.17 MeV (dashed line), and 8.45 MeV (dots).

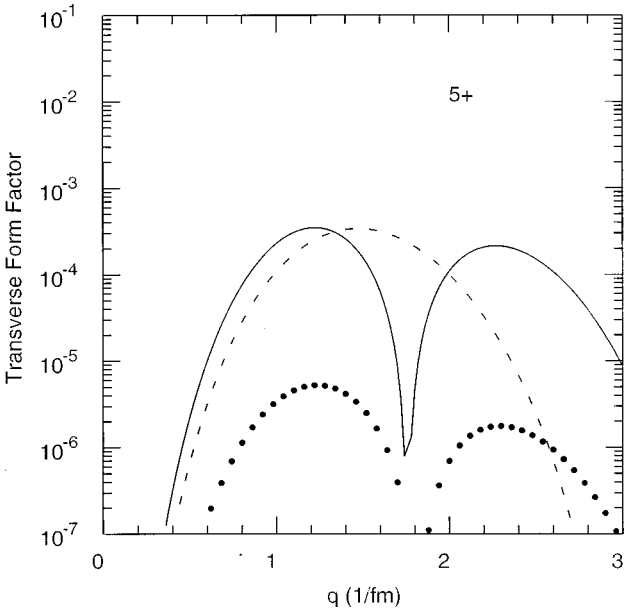

FIG. 8. Longitudinal electron scattering form factors for the lowest three 5^+ states. The levels are 5.39 MeV (solid line), 8.71 MeV (dashed line), and 9.03 MeV (dots).

is the state shown in Fig. 1) and the lower 1^+ states have 2p-2h structures.

With the effective $M1$ operator from Ref. [20], which was designed to reproduce the magnetic moments and $B(M1)$ values in the lower fp shell, the $B(M1)$ to the strong state goes down to $5.1\mu_N^2$ in better agreement with experiment. $M1$ strengths are consistent with those of McGrory and Wildenthal [5] who used a modification of the Kuo-Brown G matrix. The reduction in the experimental strength relative to the theoretical strength can be understood in terms of higher-order core-polarization plus Δ-particle admixtures [19]. The effective $M1$ operator of Towner which incorporates these effects (Table 26 of Ref. [21]) also gives 5.1 for the strong state at 11.21 MeV.

IV. RESULTS FOR THE NEUTRON-RICH Ca ISOTOPES

We are now in a position to make predictions for the more neutron-rich Ca isotopes. In Fig. 9 we show the SKX HF SPE's for the even-even nuclei as a function of mass number. One notices systematic shifts in the p states relative to the f states which are related to the change in shape of the potential as one first adds neutrons to the $f_{7/2}$ orbit up to ^{48}Ca and then begins to add neutrons to the $p_{3/2}$ and $p_{1/2}$ orbits beyond ^{48}Ca.

Although the SPE adjustments incorporated into HF* are appropriate near ^{48}Ca, as one goes toward ^{60}Ca these SPE's may change and perhaps they will become closer to the starting SKX HF values. However, lacking any experimental information on how the SPE's actually change we will simply add the same correction (the difference between the HF and D6*+HF* shown in Fig. 2) to all nuclei. These assumptions may be wrong, but they will be tested by the eventual experimental data for the most neutron-rich Ca isotopes and their comparison to the predictions.

Our procedure is to use the SPE's shown in Fig. 9 added

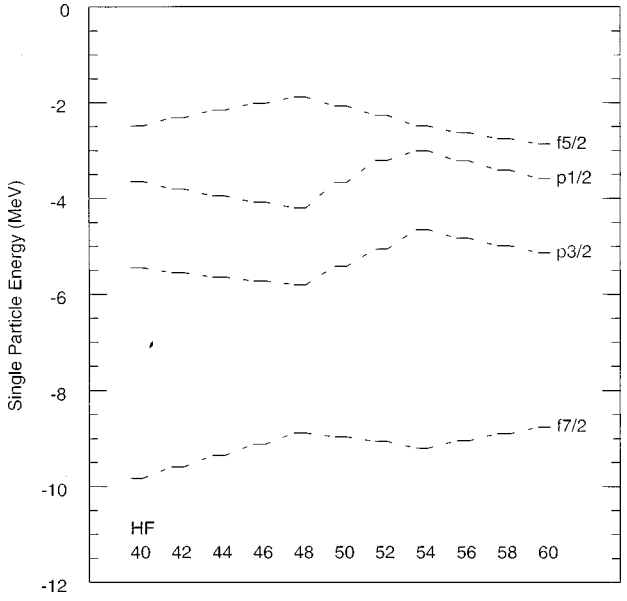

FIG. 9. The SKX HF single-particle energies as a function of mass.

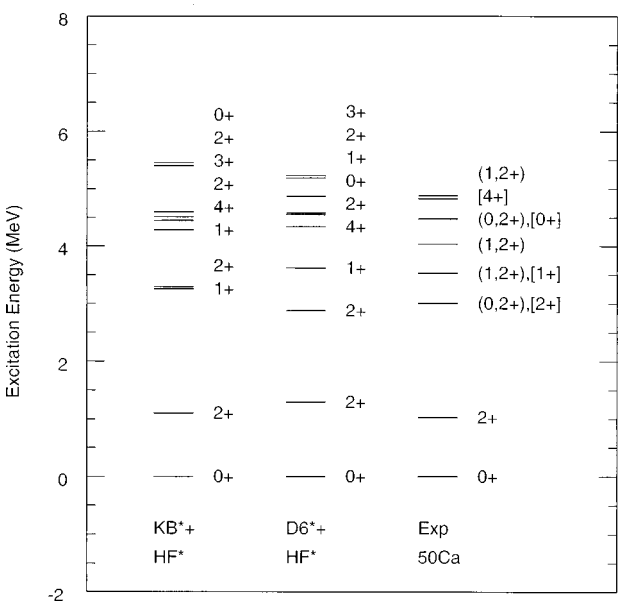

FIG. 10. Comparison of the theoretical and experimental spectra for ^{50}Ca.

with the correction for ^{48}Ca (the difference between HF and HF* in Fig. 2) for a given even-even nucleus (A) and the odd-even nucleus ($A-1$). The ''rearrangement'' energies associated with actually carrying out the HF calculation for the neighboring odd-even nuclei are small (at most a few hundred keV) compared to the uncertainties in the SM and HF interactions.

The results for the SKX (spherical) binding energy and the shell-model correlation energy are shown in Table I. The SKX binding energy is obtained from the HF calculation assuming that the neutrons fill the lowest available orbitals. The correlation energy is obtained from the difference of the full fp-shell binding energy and the lowest-energy diagonal matrix element (corresponding the configuration in which the neutrons fill the lowest available orbitals). By definition, the correlation energy is zero at the beginning and end of the shell. Such correlation energies are often considered in terms of a BCS model, and it would be interesting to compare the exact shell-model results with the BCS approximation which is often used for heavy nuclei. Although the results are in reasonable agreement with experiment, one should remember that the HF parameters (those for SKX in this case) are chosen to reproduce the ^{48}Ca binding energy under the assumption of zero correlation energy. (A typical BCS calculation gives zero for the ^{48}Ca correlation energy due to the $f_{7/2}$-subshell closure.) Thus the HF parameters should be readjusted in order to take into account the correlation energy.

TABLE I. Ground-state binding energies obtained with the D6*+HF* model.

Nucleus	SKX HF BE (MeV)	SM correlation energy (MeV)	Total BE (MeV)	Expt. BE (MeV)
^{47}Ca	406.66	0.99	407.65	406.04
^{48}Ca	415.53	1.12	416.65	415.99
^{49}Ca	421.18	1.15	422.33	421.14
^{50}Ca	426.64	1.56	428.20	427.49(1)
^{51}Ca	431.91	1.51	433.42	431.88(9)
^{52}Ca	437.01	1.85	438.86	436.6(5)
^{53}Ca	440.13	1.61	441.74	
^{54}Ca	443.16	2.45	445.61	
^{55}Ca	445.67	1.33	447.00	
^{56}Ca	448.26	1.85	450.11	
^{57}Ca	450.91	0.74	451.65	
^{58}Ca	453.63	0.88	454.51	
^{59}Ca	456.40	0.00	456.40	
^{60}Ca	459.23	0.00	459.23	

The results for ^{50}Ca are shown in Fig. 10. The experimental spins shown in parentheses are ones recently deduced from the beta decay feeding from the ^{50}K 0^- ground state [22]. The experimental spins given in square brackets are those suggested from the ^{48}Ca$(t,p)^{50}$Ca experiments [23]. The beta decay and (t,p) assignments are consistent and together provide a one-to-one correspondence with the theoretical levels.

The systematics of the energy level spectra for odd-even nuclei are shown in Fig. 11. Here we only discuss the systematics associated with the lowest level of each spin. The $7/2^-$ state in ^{47}Ca and the $3/2^-$ and $1/2^-$ states in ^{49}Ca are in agreement with experiment by the choice of the SPE's discussed in Sec. I, and as discussed there the state which is predominantly $f_{5/2}$ relative to ^{48}Ca should be associated with the second $5/2^-$ state in ^{49}Ca. The first excited $3/2^-$ state in ^{47}Ca predicted at 2.23 MeV is close to the observed state [13] at 2.01 MeV. At higher excitation energy in ^{47}Ca it is not clear which observed states should be associated with the $(fp)^7$ configurations and which are intruder states. The ground state of ^{51}Ca is tentatively assigned $3/2^-$ in agreement with the calculation. Two low-lying states at 1.24 and 1.96 MeV with unknown spins [24] could be associated with the predicted $1/2^-$ state at 1.01 MeV and the $5/2^-$ state at 1.74 MeV. (The experimental states in ^{51}Ca at lower excita-

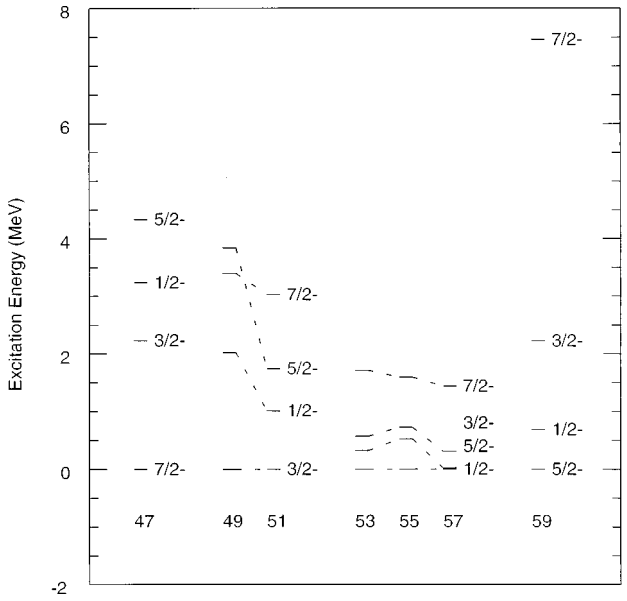

FIG. 11. Systematics of the lowest-energy states for each spin for the odd-even Ca isotopes with the D6*+HF* interaction.

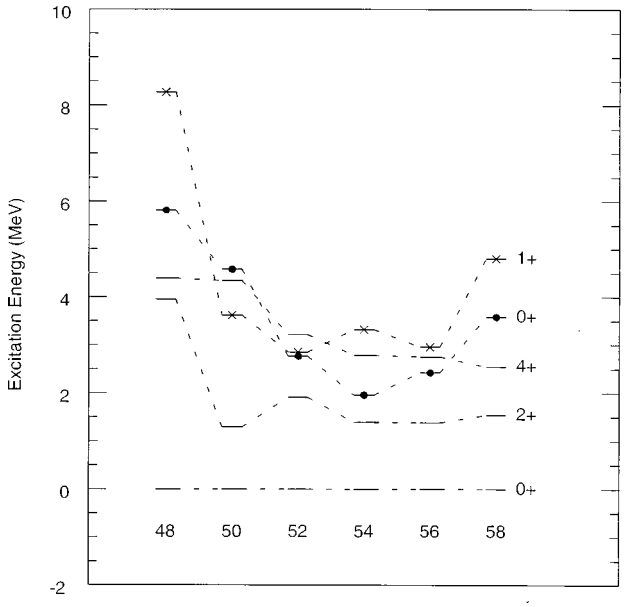

FIG. 12. Systematics of the lowest-energy states for each spin for the even-even Ca isotopes with the D6*+HF* interaction.

tion energy reported in Ref. [25] are probably spurious [24,26].)

The systematics of the energy level spectra for even-even nuclei are shown in Fig. 12. Other than those for ^{48}Ca and ^{50}Ca discussed above, the only other datum to compare with is that for the 2^+ state in ^{52}Ca which is tentatively assigned to a state at 2.56 MeV [26]. The predicted value of 1.91 MeV is somewhat low, but is higher than the 2^+ state in ^{50}Ca due to the filling of the $p_{3/2}$ subshell. The low-lying 2^+ states for $^{54-58}$Ca are due to the close spacing of the $p_{1/2}$ and $f_{5/2}$ orbitals.

V. SUMMARY AND CONCLUSIONS

In conventional shell-model calculations, the monopole terms in the Hamiltonian lead to a mass dependence of the single-particle energies which often do not agree with experiment. This leads to predictions which often diverge as the number of valence particles becomes large. The Hartree-Fock method is probably the best method for calculating the mass dependence of the single-particle energies. In particular, if one is going far from the territory established by existing data towards the most proton- and neutron-rich nuclei, the Hartree-Fock method is probably the best model for predicting the total binding energies and single-particle energies of the closed-shell nuclei.

We have demonstrated a new method for combining Hartree-Fock and large-basis shell-model calculations and tested it for the system of valence neutrons in the fp shell. The results for ^{48}Ca are very promising. With the constraint to the experimental separation energies relevant to ^{48}Ca the spectra obtained are similar for the G matrix and for the empirical (FPD6) interactions. The results are good enough to enable one to associate many more levels with experiment than has been previously possible. Predictions for the more neutron-rich Ca isotopes and their comparison to results obtainable in radioactive-beam experiments will test the present assumptions and provide insight into how they can be improved. The next step in the Hartree-Fock plus shell-model method will be to see how or if it can be extended to systems involving both neutrons and protons.

Support for this work was provided from U.S. National Science Foundation Grant No. PHY-9605207 and by the South African Foundation for Research and Development.

[1] B. A. Brown and B. H. Wildenthal, Annu. Rev. Nucl. Part. Sci. **38**, 29 (1988); B. H. Wildenthal, in *Progress in Particle and Nuclear Physics 11*, edited by D. H. Wilkinson (Pergamon, Oxford, 1984), p. 5.

[2] J. B. McGrory, B. H. Wildenthal, and E. C. Halbert, Phys. Rev. C **2**, 186 (1970).

[3] T. T. S. Kuo and G. Brown, Nucl. Phys. **A114**, 241 (1968).

[4] M. Hjorth-Jensen, T. T. S. Kuo, and E. Osnes, Phys. Rep. **261**, 125 (1995).

[5] J. B. McGrory and B. H. Wildenthal, Phys. Lett. **103B**, 173 (1981).

[6] T. Otsuka, M. Honma, and T. Mizusaki, Phys. Rev. Lett. **81**, 1588 (1998).

[7] W. E. Ormand and B. A. Brown, Phys. Rev. C **52**, 2455 (1995).

[8] A. Poves and A. Zuker, Phys. Rep. **70**, 235 (1981).

[9] B. A. Brown, W. A. Richter, R. E. Julies, and B. H. Wildenthal, Ann. Phys. (N.Y.) **182**, 191 (1988).

[10] W. A. Richter, M. G. Van der Merwe, R. E. Julies, and B. A. Brown, Nucl. Phys. **A523**, 325 (1991); L. Zhao, B. A. Brown, and W. A. Richter, Phys. Rev. C **42**, 1120 (1990).

[11] D. Vautherin and D. M. Brink, Phys. Rev. C **5**, 626 (1972).

[12] B. A. Brown, Phys. Rev. C **58**, 220 (1998).
[13] T. W. Burrows, Nucl. Data Sheets **48**, 1 (1986); **48**, 569 (1986).
[14] A. Etchegoyen, W. D. M. Rae, N. S. Godwin, W. A. Richter, C. H. Zimmerman, B. A. Brown, W. E. Ormand, and J. S. Winfield, MSU-NSCL Report No. 524, 1985.
[15] A. Novoselsky, M. Vallieres, and O. La'adon, Phys. Rev. Lett. **79**, 4341 (1997).
[16] J. H. Bjerregaard, O. Hansen, O. Nathan, R. Chapman, S. Hinds, and R. Middleton, Nucl. Phys. **A103**, 33 (1967); **A139**, 710 (1969).
[17] J. E. Wise, J. S. McCarthy, R. Altemus, B. E. Norum, R. R. Witney, J. Heisenberg, J. Dawson, and O. Schwentker, Phys. Rev. C **31**, 1699 (1985).
[18] B. A. Brown, B. H. Wildenthal, C. F. Williamson, F. N. Rad, S. Kowalski, J. Heisenberg, H. Crannell, and J. T. O'Brien, Phys. Rev. C **32**, 1127 (1985).
[19] W. Steffen, H. D. Graf, A. Richter, A. Harting, W. Wise, U. Deutschmann, G. Lahm, and R. Neuhausen, Nucl. Phys. **A404**, 413 (1983).
[20] W. A. Richter, M. G. Van der Merwe, R. E. Julies, and B. A. Brown, Nucl. Phys. **A577**, 585 (1994).
[21] I. S. Towner, Phys. Rep. **155**, 263 (1987).
[22] P. Baumann, M. Bounajma, F. Didierjean, A. Huck, A. Knipper, M. Ramdhane, G. Walter, G. Marguier, C. Richard-Serre, and B. A. Brown, this issue, Phys. Rev. C **58**, 1970 (1998).
[23] T. W. Burrows, Nucl. Data Sheets **75**, 1 (1995).
[24] Z. Chunmei, Nucl. Data Sheets **81**, 183 (1997).
[25] R. B. Firestone, V. S. Shirley, C. M. Baglin, S. Y. Frank Chu, and J. Zipkin, *Table of Isotopes* (Wiley Interscience, New York, 1996).
[26] H. Junde, H. Dailing, S. Huibin, Y. Janming, and H. Baohua, Nucl. Data Sheets **58**, 677 (1989).